

Interedge tunneling in quantum Hall line junctions

Eun-Ah Kim and Eduardo Fradkin

Department of Physics, University of Illinois at Urbana-Champaign, 1110 West Green Street, Urbana, Illinois 61801-3080

(Received 29 May 2002; published 23 January 2003)

We propose a scenario to understand the puzzling features of the recent experiment by Kang and co-workers on tunneling between laterally coupled quantum Hall liquids by modeling the system as a pair of coupled chiral Luttinger liquids with a point contact tunneling center. We show that for filling factors $\nu \sim 1$ the effects of the Coulomb interactions move the system deep into the strong-tunneling regime, by reducing the magnitude of the Luttinger parameter K , leading to the appearance of a zero-bias differential conductance peak of magnitude $G_t = Ke^2/h$ at zero temperature. The abrupt appearance of the zero-bias peak as the filling factor is increased past a value $\nu^* \gtrsim 1$, and its gradual disappearance thereafter can be understood as a crossover controlled by the main energy scales of this system: the bias voltage V , the crossover scale T_K , and the temperature T . The low height of the zero-bias peak $\sim 0.1e^2/h$ observed in the experiment and its broad finite width can be understood naturally within this picture. Also, the abrupt reappearance of the zero-bias peak for $\nu \gtrsim 2$ can be explained as an effect caused by spin-reversed electrons, i.e., if the 2DEG is assumed to have a small polarization near $\nu \sim 2$. We also predict that as the temperature is lowered ν^* should decrease, and the width of the zero-bias peak should become wider. This picture also predicts the existence of a similar zero-bias peak in the spin tunneling conductance near for $\nu \gtrsim 2$.

DOI: 10.1103/PhysRevB.67.045317

PACS number(s): 73.23.-b, 71.45.Lr, 72.15.-v

I. INTRODUCTION

The properties of the edge states of two-dimensional electron gases (2DEG's) in high magnetic fields reflect the structure of the Hilbert spaces of bulk fractional and integer quantum Hall (FQH) states. In the absence of edge reconstruction, the low-energy Hilbert spaces of the FQH edge states can be represented by a suitable set of chiral Luttinger liquids.¹⁻³ This identification brought considerable interest in the study of FQH edge states as a well-controlled laboratory for experimental exploration of the quantum transport properties of Luttinger liquids. Much effort has been devoted to the theoretical^{4,5} and experimental study of tunneling of both between FQH edge states⁶ and into FQH edge states.⁷ Measurements⁷ of electron tunneling from a bulk-doped GaAs electron into the sharp edge of a FQH state with filling fractions $\nu \leq 1$ have confirmed the existence of both the scaling regime^{4,5} and the crossover behavior⁸ predicted by the chiral Luttinger liquid picture. However, many important open questions remain about the actual observed behavior of the tunneling exponent and its consistency with the physics of the bulk FQH states (see, for instance, Refs. 4 and 9-11, and references therein).

Recently, Kang and co-workers¹² have measured the differential tunneling conductance of a device in which two 2DEG's in the integer quantum Hall regime are laterally coupled through an atomically precise tunneling barrier. Their data show a very sharp and intense differential conductance peak of height $G_t \equiv dI_t/dV \approx 0.1e^2/h$ at zero bias for certain ranges of magnetic field on top of an oscillatory behavior, which appears in qualitatively the same manner for all ranges of magnetic field. The data show an abrupt appearance and the following gradual disappearance of the zero-bias conductance (ZBC) peak as the filling factor is increased past the apparent threshold values $\nu_1^* \gtrsim 1$ and $\nu_2^* \gtrsim 2$, respectively. In both cases, the height of the ZBC peak they ob-

served is considerably smaller than the quantum of conductance e^2/h and the ZBC peak was observed over a fairly broad range of filling fractions ($\lesssim e^2/2h$). The data of Kang *et al.*¹² show no ZBC peak in the tunneling conductance for $\nu \leq 1$.

The theoretical explanation of the experiment of Kang and co-workers has focused on the fact that it is not possible to tunnel electrons between two perfectly aligned FQH edges with opposite chirality.² Thus, if the barrier is assumed to be atomically precise, the only way in which tunneling can possibly take place is by the anticrossing of Landau levels belonging to both sides of the barrier.¹³ In the Landau gauge $\vec{A} = (0, Bx, 0)$, where the x direction is chosen perpendicular to the barrier and the y direction along the barrier, the single-particle wave function has the form $\varphi(x, y) = \exp(iky)\phi_k(x)$ where $\phi_k(x)$ is an eigenfunction of the Hamiltonian

$$H_k(x) = -\frac{\hbar^2}{2m} \frac{\partial^2}{\partial x^2} + \frac{1}{2} m \omega_c^2 (x - kl^2)^2 + V_B(x), \quad (1)$$

with $V_B(x)$ a potential due to the barrier which is symmetric about $x=0$. The dispersion curves originating from the two systems on both sides of the barrier overlap around $k=0$. At the crossing points, gaps open as a consequence of a coupling between the counterpropagating edge states.¹³ This is indeed the scenario assumed in the work of Kang and co-workers¹² and by Mitra and Girvin,¹⁴ Lee and Yang,¹⁵ Kollar and Sachdev,¹⁶ and by an earlier calculation by Takagaki and Ploog.¹⁷

In this picture, the appearance of a zero-bias conductance peak is ascribed to the existence of a gap in the spectrum of edge states at the barrier, since a gap suppresses the conduction channel along the barrier provided by unmixed edge states with opposite chirality formed by the barrier. Mitra and Girvin,¹⁴ as well as Kollar and Sachdev,¹⁶ observed that

electron-electron interactions yield a substantial modification of the gap which cannot be accounted for by level mixing arguments. In these theories, the gap is equal to the soliton energy of a quantum sine-Gordon model, derived from a microscopic theory of the barrier. Notice that, due to the Landau level mixing induced by the barrier, the effective Fermi wave vector of the barrier states is $k_F=0$. Thus a gap in the spectrum does not require backscattering in this geometry. In particular, Mitra and Girvin¹⁴ used a Hartree-Fock theory to calculate the Luttinger liquid parameter, the collective mode velocity, and the momentum cutoff of the effective sine-Gordon theory. It was found that the Coulomb interaction, which is taken into account in Hartree-Fock theory, leads to a substantial enhancement of the gap. More recently, Kollar and Sachdev,¹⁶ used a method of matched asymptotics to determine the momentum cutoff for sine-Gordon theory. The gap they found is larger than the result of Mitra and Girvin.

However, even with the gap obtained by Kollar and Sachdev¹⁶ it is not possible to understand the height of the zero-bias conductance peak. Both Refs. 14 and 16 predict on general grounds a zero-bias peak with height e^2/h , larger than the experimental result $0.1e^2/h$ of Ref. 12 by approximately one order of magnitude. Furthermore, in this picture the ZBC peak is expected above the second Landau level in the noninteracting system, whereas the peak region was prominent near $\nu^*\approx 1$ in the experiment. (Interaction effects do not modify this result in any essential way.) Given these facts it was argued in Refs. 14 and 16 that effects of disorder may be ultimately responsible for these discrepancies between theory and experiment.

In search of an answer to these questions, we reexamined the alternative scenario of tunneling between countercirculating edge states through an imperfection of the tunneling barrier. We were motivated partly by the observation that the effects of anticrossing induced by the barrier are not expected to occur at least before the second Landau level begins to be filled, which is not the regime in which the zero-bias peak first appears. Thus we will assume the more standard situation of a barrier separating two FQH states with edges of opposite chirality and nonvanishing Fermi wave vectors. Under these circumstances tunneling is only allowed if impurities and imperfections are present. This is a possibility that must be considered seriously particularly given that in the end impurity scattering is invoked as the explanation for the magnitude of the zero-bias peak, as advocated in Refs. 14 and 16. Thus, in this paper we will assume that the barrier is precise enough to have just a few imperfections which act as weak tunneling centers. In fact we will assume that there is just one such tunneling center.

In the situation of the experiment of Kang *et al.*, where right- and left-moving edges were spatially separated by a barrier, a local deformation of the edges due, for instance, to an impurity can result in a weak tunneling center which mimics the pinch-off effect of the patterned back gate electrode of the experiment by Milliken, Umbach, and Webb.⁶ The authors of Ref. 6 have observed expected temperature dependence of the tunneling conductance through the point contact^{18,19} for $\nu=1/3$. However, a quite unique feature of

the setup of Ref. 12 is that it can explore not only the effect of backscattering through a (presumably) point contact, but also the effects of electron-electron interactions along the edges.

Our analysis shows that the electron-electron interaction plays a crucial role in the tunneling conductance. Electron-electron interactions turn the pair of edge states into a single nonchiral Luttinger liquid with an effective Luttinger parameter $K<1$ for filling factors $\nu\geq 1$. This problem can be mapped onto the problem of a junction in a Luttinger liquid first studied by Kane and Fisher,^{4,5} with a Luttinger parameter reduced from 1 due to the effects of the Coulomb interactions along the barrier, which brings the system to the strong-tunneling phase if it were at $T=0$. In Refs. 4 and 5, Kane and Fisher pointed out that for $K<1$, tunneling at a point contact is a relevant perturbation and the system flows to a strong-coupling regime. While $K<1$ suggests that the threshold for a zero-bias peak should be observed at a filling factor somewhat below $\nu=1$, we find that there is a non-trivial temperature dependence of the height and width of the zero-bias peak induced by the renormalization flow of the tunneling operator.

We studied the effects of finite temperature by mapping the problem to the boundary sine-Gordon (BSG) problem which is exactly solvable. By combining a number of known exact results of the BSG theory with the calculation of an appropriate renormalization group β function, we suggest a natural explanation of the salient features of the experiment of Ref. 12. We studied in detail the crossover behavior of the tunneling conductance as a function of temperature and found that it can explain qualitatively the observations of Ref. 12. We find that finite temperature is responsible for both the low height of the peak and its gradual disappearance when the filling factor is increased past $\nu\sim 1$. Further experimental studies of the temperature dependence of the zero-bias peak can check these theoretical predictions. In particular we give an explicit expression for the temperature dependence of the differential conductance at zero bias voltage for the particular value of the Luttinger parameter $K=1/2$. For more general values of the Luttinger parameter the solutions are more complicated but nevertheless vary smoothly and slowly with K (see below). Although the data that have been published so far of the experiment of Kang and co-workers¹² are at a temperature of 300 mK, unpublished data from the same group in the temperature range from 300 mK to 8 K are well described by our results.²⁰

We have also studied tunnel junctions at a barrier in partially spin-polarized QH states. We find that the reappearance of the peak region near $\nu\sim 2$ can be explained if the electron gas is not fully polarized but instead has a small spin polarization. We also consider in this paper the interesting case of a line junction in a spin-singlet $\nu=2$ state. We find that for these QH states, at $\nu\geq 2$ a spin-spin interaction across a single point junction leads to a number of interesting effects in both spin and charge transport across the junction.

This paper is organized as follows. In Sec. II, we introduce the model for a IQH-barrier-IQH junction with a single tunneling center and bosonize the model. In Sec. III we map the model to the integrable BSG model by using a standard

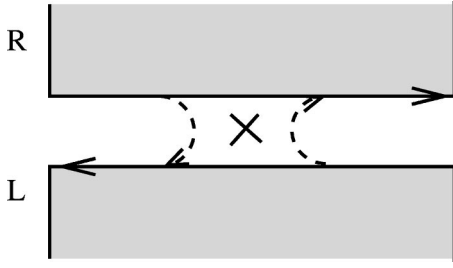


FIG. 1. A line junction with a single backscattering center. The two shaded regions and the space between correspond, respectively, to two regions of 2DEG of widths 13 and 14 μm and the 88- \AA -thick $\text{Al}_{0.1}\text{Ga}_{0.9}\text{As}/\text{AlAs}$ barrier of 2DEG-barrier-2DEG junctions used by Kang *et al.* The single tunneling center is represented by a cross in the figure. The system is equivalent to a one-dimensional Fermi system with right- and left-moving branches, interacting with each other through short-range interactions.

folding procedure. The result will be used to understand the experiment near $\nu=1$. In Sec. IV we propose an explanation for the experimental results near $\nu=2$ with the assumption that there is a small spin polarization for $\nu=2$. Here we generalize our analysis and discuss the role of exchange, Zeeman, and magnetic anisotropy interactions on the tunneling processes. Finally, in Sec. V we review our main results and give some predictions on future experiments based on our analysis.

II. MODEL HAMILTONIAN

We begin by briefly describing the experimental setup (see Fig. 1) and the most salient results of Ref. 12. The 2DEG-barrier-2DEG junctions used by Kang *et al.*¹² consisted of two regions of 2DEG of widths 13 and 14 μm , where the electrons reside in the two-dimensional interface of the GaAs-AlGaAs heterostructure, separated by a 88- \AA -thick $\text{Al}_{0.1}\text{Ga}_{0.9}\text{As}/\text{AlAs}$ barrier of height 220 meV. These junctions are believed to be atomically precise, which means that they have very few defects on their entire length. In the experiment the conductance at $T=300$ mK showed an oscillatory behavior as a function of bias voltage with successive peaks spaced by an energy of the order of the cyclotron energy $\hbar\omega_c$ in the full range of magnetic field. This effect suggests that there is a mixing between Landau levels enabled by a level shift due to large bias voltage. However, for fillings $\nu=n\hbar/eB \geq 1$ and $\nu \geq 2$, a sharp conductance peak dominates at zero bias. The peak heights were $0.12e^2/h$ and $0.11e^2/h$, respectively, for the samples published, but the height typically varies from sample to sample, always being of the order of $0.1e^2/h$.²⁰

The model Hamiltonian for the setup of the experiment of Kang and co-workers that we will use here is a variant of the one considered by Kane and Fisher.^{4,5} We will make the simplifying assumption the electron-electron interactions at the barrier are sufficiently well screened so that they can be represented by effective short-range intraedge and interedge interactions. While this assumption is not fully justified it represents a minor change to the physics of the system. Thus, the effects of the width of the barrier are included in the

matrix element. The right- and left-moving branches represent the edge states of two $\nu=1$ QH states laterally coupled by the barrier. These edges have nonvanishing Fermi wave vectors equal in magnitude (for a symmetric barrier) and with opposite direction, indicating the chiral nature of the edge states. Backscattering is forbidden everywhere due to momentum conservation, and in the absence of a periodic potential there is no umklapp scattering. The electron-electron interactions are thus purely due to “forward scattering” both intraedge and interedge, which conserve chirality. Thus, under these assumptions, the pair of edge states behaves effectively like a single nonchiral one-dimensional Luttinger liquid, with an effective velocity v_0 and an effective Luttinger coupling constant g_c . The main effect of the impurity is to provide for a backscattering center at the impurity site which we will define to be the origin, $x=0$ (see Fig. 1). The model that we will discuss and solve for two coupled $\nu=1$ edges with opposite chirality can be easily extended to discuss the same issues for fractional quantum Hall states. However, for reasonable values of the dimensionless coupling constant (defined below) the resulting effective Luttinger parameter is always in the range $K>1$ in which tunneling is suppressed and no ZBC peak can be observed. Thus, for the rest of this paper we will restrict our discussion to the case $\nu>1$ in which there are no fractional quantum Hall states (for fully polarized systems).

The system can thus be treated as if it were effectively one dimensional, i.e., as if the right- and left-moving branches overlapped with each other and were coupled via a screened Coulomb interaction. Following Wen’s hydrodynamic approach,^{2,19} the edge states of oppositely moving modes are described in terms of normal-ordered right- and left-moving densities J_{\pm} which satisfy equal-time commutation relations in the form of a $U(1)$ Kac-Moody algebra:

$$[J_{\pm}(x), J_{\pm}(x')] = \mp \frac{i}{2\pi} \partial_x \delta(x-x'). \quad (2.1)$$

The Hamiltonian density for the line junction may be written as a sum of two terms $\mathcal{H}=\mathcal{H}_G+\mathcal{H}_t$, where \mathcal{H}_G includes the effects of both interedge and intraedge interactions, and \mathcal{H}_t represents tunneling term at $x=0$. \mathcal{H}_G is given by

$$\mathcal{H}_G = \pi v_0 (J_-^2 + J_+^2 + 2g_c J_+ J_-), \quad (2.2)$$

where we assumed the speed of right- and left-moving electrons to be same with v_0 , and the third term stands for the density-density interaction between chiral electrons.

The dimensionless coupling constant g_c , which measures the strength of the interaction, can be estimated to be $g_c \sim U/E_F$ where, for the case of Coulomb interactions, $U \equiv e^2/\epsilon d$ where d is the effective distance between the two edges, ϵ is the static dielectric constant, and E_F is the Fermi energy for the edge states, assumed to be the same on both sides of the barrier. It is important to keep in mind that in practice there is no reliable way to determine g_c in terms of microscopic parameters. Still, this lowest-order estimation implies that the Coulomb interaction must be fairly strong in the actual experimental setup. In any case, we expect that the dimensionless coupling constant g_c should be a smooth func-

tion of the bulk filling factor ν and of the thickness of the barrier. Intuitively we expect that as the filling factor increases, either by raising the electron density or by decreasing the magnetic field, the effective distance between the edges of the two quantum Hall liquids will decrease. Consequently we expect that the dimensionless coupling constant g_c will increase as the filling factor increases. We will see below that this effect will play an important role in the explanation of the effects seen in the experiments of Kang and co-workers.¹²

We will represent the effects of backscattering at the tunneling center (at the origin) by a local tunneling operator which in terms of right- and left-moving electron creation and annihilation operators has the standard form

$$\mathcal{H}_t = t(\psi_+^\dagger \psi_- + \psi_-^\dagger \psi_+) \delta(x), \quad (2.3)$$

where t is the tunneling amplitude.

We will solve this problem using the standard bosonization approach.²¹ The right- and left-moving chiral Fermi fields are bosonized according to the Mandelstam formulas

$$\psi_\pm^\dagger(x) \propto \frac{1}{\sqrt{2\pi}} e^{\pm i\phi_\pm(x)}, \quad (2.4)$$

where ϕ_\pm are chiral right- and left-moving Bose fields, respectively. In the notation of Ref. 8, the Lagrangians for the decoupled edges are

$$\mathcal{L}_\pm[\phi_\pm] = \frac{1}{4\pi} \partial_x \phi_\pm (\pm \partial_t - v_0 \partial_x) \phi_\pm. \quad (2.5)$$

The normal-ordered density operators are bosonized according to the rules

$$J_\pm = -\frac{1}{2\pi} \partial_x \phi_\pm. \quad (2.6)$$

In terms of the chiral boson fields ϕ_\pm , the full (bosonized) Lagrangian density is

$$\begin{aligned} \mathcal{L} = & \frac{1}{4\pi} \partial_x \phi_+ (\partial_t - v_0 \partial_x) \phi_+ + \frac{1}{4\pi} \partial_x \phi_- (-\partial_t - v_0 \partial_x) \phi_- \\ & - \frac{2g_c}{4\pi} \partial_x \phi_+ \partial_x \phi_- - \delta(x) \Gamma \cos(\phi_+ + \phi_-), \end{aligned} \quad (2.7)$$

where Γ measures the tunneling amplitude. As usual, this system is diagonalized by the (Bogoliubov) transformation

$$\begin{aligned} \phi_+ &= \frac{K+1}{2\sqrt{K}} \varphi_+ + \frac{K-1}{2\sqrt{K}} \varphi_-, \\ \phi_- &= \frac{K-1}{2\sqrt{K}} \varphi_+ + \frac{K+1}{2\sqrt{K}} \varphi_-, \end{aligned} \quad (2.8)$$

and the choice of K that diagonalizes the system is the effective Luttinger parameter. Letting v denote the renormalized velocity, respectively, the effective Luttinger parameter and the renormalized velocity are given respectively by

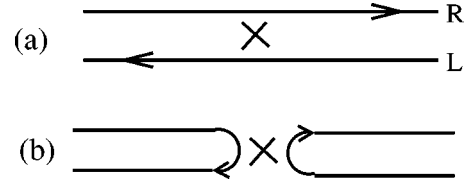


FIG. 2. Two phases for the system described by the Lagrangian density, Eq. (2.10), depending on the value of the Luttinger parameter K defined by Eq. (2.9) at $T=0$. There is a quantum phase transition at $K=1$ between two phases (Ref. 4). (a) A perfectly conducting regime for $K>1$, which corresponds to no tunneling in our problem, and (b) a perfectly insulating regime for $K<1$, which corresponds to the perfect tunneling in our problem.

$$K \equiv \sqrt{\frac{1-g_c}{1+g_c}}, \quad v \equiv v_0 \sqrt{1-g_c^2}. \quad (2.9)$$

With these definitions the Lagrangian density for the line junction with a point contact at $x=0$ becomes

$$\begin{aligned} \mathcal{L} = & \frac{1}{4\pi} \partial_x \varphi_+ (\partial_t - v \partial_x) \varphi_+ + \frac{1}{4\pi} \partial_x \varphi_- (-\partial_t - v \partial_x) \varphi_- \\ & - \delta(x) \Gamma \cos[\sqrt{K}(\varphi_+ + \varphi_-)]. \end{aligned} \quad (2.10)$$

By comparison with Ref. 8 we see that the Luttinger parameter K plays the role of an effective inverse filling factor $\bar{\nu} = 1/K$. With the notation that we are using here K plays the role of the constant g defined in Ref. 4.

Kane and Fisher studied transport properties of a one-dimensional electron gas with a single impurity in Ref. 4 and predicted a change in the nature of the transport across the point contact (the impurity) at $T=0$ depending on the value of Luttinger parameter K , finding perfect transmission for $K>1$ and perfect insulating behavior for $K<1$ due to a complete backscattering at the impurity; see Fig. 2.

As discussed in the caption of Fig. 2, perfect conduction along the wire in the Kane-Fisher problem^{4,5} corresponds to conduction *only* along the barrier in our problem and, hence, to the complete suppression of tunneling across junction in our case and vice versa. However, we should keep in mind that the expression of Eq. (2.9) can be the correct expression for the Luttinger parameter only when the dimensionless coupling constant g_c in Eq. (2.2) is small. From our previous estimation of g_c we found that to lowest order in U/E_F , g_c is substantially large. Hence the effects of irrelevant operators not included in the Hamiltonian H cannot be ignored as they will give rise to finite, and presumably not small, corrections to the functional dependence of the Luttinger parameter K on the dimensionless Coulomb interaction g_c . Nevertheless, what matters is that even after all these corrections are accounted for there is an effective Luttinger parameter K , albeit with a complicated but analytic dependence on microscopic parameters. Thus we can still define an effective coupling constant \tilde{g}_c through an identity of the form $K \equiv \sqrt{(1-\tilde{g}_c)/(1+\tilde{g}_c)}$, where $\tilde{g}_c(\nu) = f(g_c(\nu)) = g_c(\nu) + O(g_c^2)$. Therefore all we can tell from Eq. (2.9) is that the Luttinger parameter will become substantially smaller than 1

due to Coulomb interaction effects. However, what matters here is that this condition is sufficient to bring the junction deep into the backscattering phase at zero temperature where backscattering is a strongly relevant perturbation. In this regime the perturbative approach of Kane and Fisher⁴ is not enough to determine the transport properties at finite temperature. Fortunately, this problem can be mapped to an exactly solvable boundary sine-Gordon problem which will enable us to go beyond the perturbative regime. We analyze the problem from the perspective of BSG theory in the next section.

III. TUNNELING CONDUCTANCE NEAR $\nu=1$

A. Mapping to the boundary sine-Gordon model

In order to make contact with the results of Fendley, Ludwig, and Saleur, we will now map the effective Lagrangian of Eq. (2.10) to the boundary sine-Gordon theory. To that effect we will perform a parity operation $x \rightarrow -x$ acting only on the left-moving field φ_- by which it now becomes a right-moving chiral boson, still denoted by φ_- . Let us define the even and odd linear combinations of (right-moving) chiral fields

$$\begin{aligned}\varphi_e &= \frac{1}{\sqrt{2}}(\varphi_+ + \varphi_-), \\ \varphi_o &= \frac{1}{\sqrt{2}}(-\varphi_+ + \varphi_-),\end{aligned}\quad (3.1)$$

in terms of which the Lagrangian takes the simpler, decoupled, form

$$\begin{aligned}\mathcal{L} &= \frac{1}{4\pi} \partial_x \varphi_e (\partial_t - v \partial_x) \varphi_e + \frac{1}{4\pi} \partial_x \varphi_o (\partial_t - v \partial_x) \varphi_o \\ &\quad - \delta(x) \Gamma \cos[\sqrt{2K} \varphi_e].\end{aligned}\quad (3.2)$$

In terms of the right-moving chiral bosons φ_e and φ_o , the edge currents J_{\pm} become

$$\begin{aligned}J_+ &= + \frac{K}{2\pi\sqrt{2K}} \partial_x \varphi_o - \frac{1}{2\pi\sqrt{2K}} \partial_x \varphi_e, \\ J_- &= + \frac{K}{2\pi\sqrt{2K}} \partial_x \varphi_o + \frac{1}{2\pi\sqrt{2K}} \partial_x \varphi_e.\end{aligned}\quad (3.3)$$

In the presence of the point contact, the current along the junction splits into a backscattering or tunneling current and a forward-scattering or transmitted current. The tunneling current $J_t = J_+ - J_-$ is given by

$$J_t = - \frac{1}{2\pi} \sqrt{\frac{2}{K}} \partial_x \varphi_e, \quad (3.4)$$

and it depends only on the chiral boson φ_e .

In order to map the problem to the boundary sine-Gordon theory we will use the standard folding procedure.^{22–26} Let $x_0 = vt$ denote a rescaled time coordinate and $x_1 = x$. We

map each of left-moving fields defined on the whole line φ_e and φ_o to nonchiral fields Φ_e and Φ_o defined on the half-line $x_1 \geq 0$. These nonchiral fields are decomposed into their right- and left-moving parts:

$$\begin{aligned}\Phi_e(x_0, x_1) &= \Phi_{e,-}(x_1 + x_0) + \Phi_{e,+}(-x_1 + x_0), \\ \Phi_o(x_0, x_1) &= \Phi_{o,-}(x_1 + x_0) + \Phi_{o,+}(-x_1 + x_0),\end{aligned}\quad (3.5)$$

where the right-moving parts of the Φ fields come from the $x_1 > 0$ parts of the φ fields, and the left-moving parts of the Φ fields come from the $x_1 < 0$ parts of the φ fields:

$$\begin{aligned}\Phi_{e,+}(x) &\equiv \varphi_e(x) & \Phi_{o,+}(x) &\equiv \varphi_o(x) & \text{for } x_1 > 0, \\ \Phi_{e,-}(x) &\equiv \varphi_e(x) & \Phi_{o,-}(x) &\equiv -\varphi_o(x) & \text{for } x_1 < 0,\end{aligned}\quad (3.6)$$

with $\Phi_{e/o,+} = 0$ for $x_1 < 0$ and $\Phi_{e/o,-} = 0$ for $x_1 > 0$. In terms of the Φ fields, the Lagrangian density on the whole line of Eq. (3.2) is mapped onto a Lagrangian density on the half-line $x_1 \geq 0$,

$$\mathcal{L} = \frac{1}{8\pi} (\partial_\mu \Phi_e)^2 + \frac{1}{8\pi} (\partial_\mu \Phi_o)^2 - \delta(x_1) \frac{\Gamma}{v} \cos\left(\sqrt{\frac{K}{2}} \Phi_e\right). \quad (3.7)$$

In Eq. (3.7), the odd boson Φ_o remains free, simply obeying Neumann boundary conditions at the origin $\Phi_o(x_1=0) = 0$, and decouples. In contrast, the even field Φ_e , which from now on will be denoted by Φ for simplicity, has a nontrivial dynamics governed by the Lagrangian density

$$\mathcal{L} = \frac{1}{8\pi} (\partial_\mu \Phi)^2 - \delta(x_1) \frac{\Gamma}{v} \cos\left(\sqrt{\frac{K}{2}} \Phi\right) \quad (3.8)$$

defined for $x_1 \geq 0$. The (even) field Φ and obeys Neumann boundary conditions at both $x_1 = 0$ and $x_1 \rightarrow \infty$.

The action of Eq. (3.8) is known as the boundary sine-Gordon model and is a well-studied integrable quantum field theory.²⁷ It is a theory of a free scalar field coupled to the vertex operator $\mathcal{O} = \exp[i\sqrt{K/2}\Phi(0,t)]$ at the boundary. The main physical effect of the tunneling operator is to induce a flow of boundary conditions²⁸ (BC's) at $x_1 = 0$: for $\Gamma = 0$, Φ obeys a Neumann BC at $x_1 = 0$, whereas for $\Gamma \rightarrow \infty$ Φ has a Dirichlet BC at $x_1 = 0$. The (boundary) scaling dimension for the operator \mathcal{O} at the weak-coupling fixed point $\Gamma \rightarrow 0$ is $d_{\mathcal{O}} = 2(\sqrt{K/2})^2 = K$. Thus for $K < 1$, as in our case, the tunneling operator is relevant and the weak-coupling fixed point is unstable. Conversely, in this regime the strong-coupling fixed point is stable. On the other hand, for $K > 1$, \mathcal{O} is irrelevant at the weak-coupling fixed point and the system is more appropriately described by a dual picture as in the case discussed in Ref. 8. This is the conventional situation in the fractional quantum Hall regime. In our case, the Coulomb interaction reduced the value of K to be smaller than 1, leading to a situation similar to the one considered by Fendley and co-workers,²² who investigated the problem of interedge quasiparticle tunneling in a FQH state.

We note in passing that in general, as noted in Ref. 22, $4k_F$ processes should be fine-tuned to zero if $1/9 < K < 1/4$

for the system to be integrable. (This is so because only one relevant perturbation is allowed for integrability.²⁷) Fortunately in the case of interest here $4k_F$ processes are forbidden in a chiral system with only one tunneling center. Hence the system we are interested in is automatically fine-tuned and the problem is integrable even for $K < 1/4$.

The (massless) boundary sine-Gordon theory, regarded as the massless limit of the conventional bulk sine-Gordon theory, was shown to be integrable by Goshal and Zamolodchikov,²⁷ who also determined the spectrum of the BSG system by means of the thermodynamic Bethe ansatz (TBA) for an arbitrary value of the Luttinger parameter K . The spectrum contains a kink and an antikink and $n-2$ breathers for $n-1 < 1/K \leq n$. The case $K=1/2$ is special in that there is no breather and the even boson theory can be represented in terms of free fermions. In this case, kinks and antikinks are just particle-hole transforms of ordinary fermions. Although this problem is solvable for any value of K , the TBA computation is much simpler for $1/K = m$, where m is an integer (in this case the bulk scattering matrix is completely diagonal.) Since we are interested in the regime $K < 1$, we will focus in what follows on the case $K = 1/m$, with integer m .

In the problem of transport through a point contact with $1/K$ integer there is a dynamically generated scale T_K which uniquely determines the low-energy physics.^{8,22,29} (In this problem T_K plays a role similar to the Kondo temperature in the conventional Kondo problem of a magnetic impurity in a metallic host.) The scale T_K is a function of the point-contact interaction strength Γ and of the ultraviolet cutoff scale Λ . T_K is an energy scale separating the low-energy, long-distance regime (IR regime) and the high-energy, short-distance regime (UV regime); T_K can also be viewed as the temperature at which the weak-coupling expansion breaks down. One of the fundamental properties of quantum impurity problems like point-contact tunneling or the Kondo model is that observables, such as the differential conductance in the point-contact problem or the magnetic susceptibility in the Kondo problem, are described in the scaling regime by universal scaling functions of the temperature T , the bias voltage V (H/T for the Kondo model), the coupling constant Γ , and the (ultraviolet) cutoff Λ , of the form

$$G(\Lambda, V, T, \Gamma) \xrightarrow{T, V \ll \Lambda} G(T/T_K, V/T), \quad (3.9)$$

where the dependence of conductance upon cutoff and interaction strength is hidden in the definition of T_K .^{23,26} Fendley and co-workers²² find a dependence of T_K on Γ of the form

$$T_K = C\Gamma^{1/(1-K)}, \quad (3.10)$$

where C is a nonuniversal constant.

The rest of this section will be devoted to an analysis of the implications of the known results for the BSG model to the tunneling contact problem that we are interested in and to its implications for the experiment of Kang and co-workers.¹² It will be shown that both the Coulomb interaction and finite temperature play important role in the behavior of the zero-bias conductance peak near $\nu \sim 1$.

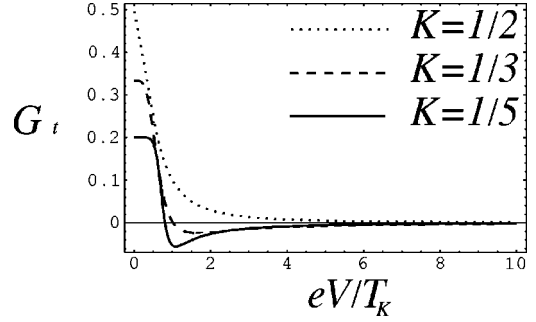


FIG. 3. The differential tunneling conductance at zero temperature vs eV/T_K . Each dotted, dashed, and solid line represents $K = 1/2$, $K = 1/3$, and $K = 1/5$, respectively. All three curves share the common feature of a rapid increase in the G_t as the voltage is lowered past T_K followed by the saturation of G_t to the value determined by the Luttinger parameter Ke^2/h at $V/T_K = 0$.

B. Comparison with the experiment

We have shown above that the problem of the point contact in two laterally coupled FQH liquids maps onto the boundary sine-Gordon theory. In particular we showed that the effective Luttinger parameter K plays the role of an effective inverse filling factor. In this picture the point contact maps onto the problem of the tunneling of electrons between two edges with filling factor $\bar{\nu} = 1/K > 1$. Fendley, Ludwig, and Saleur²² (FLS) solved a very similar problem but in the regime $\bar{\nu} < 1$. FLS also found that, at $T=0$ and voltage V , the tunneling current I obeys the exact remarkable duality

$$I(T_K, V, \bar{\nu}) = \frac{e^2}{h} \bar{\nu} V - \bar{\nu}^2 I(T_K, V, \bar{\nu}^{-1}). \quad (3.11)$$

Using this result we find that the differential tunneling conductance at zero temperature for our problem is given by^{22,30}

$$G_t = K \frac{e^2}{h} \times \begin{cases} 1 - \sum_{n=1}^{\infty} c_n(K^{-1}) \left(\frac{eV}{T_K}\right)^{2n(K^{-1}-1)} & \frac{eV}{T_K} < e^\delta, \\ \sum_{n=1}^{\infty} c_n(K) \left(\frac{eV}{T_K}\right)^{2n(K-1)} & \frac{eV}{T_K} > e^\delta, \end{cases} \quad (3.12)$$

where the coefficients c_n are defined as

$$c_n(K) = (-1)^{n+1} \frac{\Gamma(nK+1)}{\Gamma(n+1)} \frac{\Gamma(1/2)}{\Gamma(n(K-1)+1/2)}, \quad (3.13)$$

where $\Gamma(z)$ is the gamma function. (Here $\delta = [K \ln K + (1-K) \ln(1-K)]/[2(1-K)]$ is a parameter that determines the radii of convergence of these series.)

In Fig. 3 we plot G_t at zero temperature for different values of K as functions of eV/T_K (in units of e^2/h). We can see from the plot that the differential conductance increases rapidly as the voltage is lowered below T_K and that it saturates rather rapidly to a value determined by the Luttinger parameter Ke^2/h at $V/T_K = 0$ at zero temperature. Recall that Eq. (3.12) is valid only for $K < 1$ where the tunneling operator is relevant.³¹ The experiments of Kang and co-workers

are done in the regime $\nu \geq 1$. Thus here we consider the edge states of two nominally $\nu=1$ quantum Hall states but take into account the effects of the interedge interactions which make the Luttinger parameter $K < 1$. In the fractional regime the bare value of K is greater than 1, and it is reduced in value by the interedge interactions. Thus there exists a critical filling factor (or magnetic field) $\nu_c(g_c)$ at which $K=1$. For $\nu > \nu_c$ we have $K < 1$ while for $\nu < \nu_c$ we have $K > 1$. Therefore when the filling factor is increased past ν_c , the tunneling operator becomes relevant and the tunneling amplitude Γ flows to infinity (which makes T_K grow to infinity as well), leading to a finite conductance at all bias voltages at zero temperature. We note here that the theory presented in this paper, based as it is on a single chiral boson with compactification radius 1 per edge, does not formally apply in the fractional quantum Hall regime. Up to important subtleties which involve either additional neutral or topological edge modes (see, for instance, Refs. 9–11), the fractional regime can be viewed as a theory of two coupled effective charge bosons, each with radius $\sqrt{\nu}$, and an effective Luttinger parameter $K_{\text{eff}} = K/\nu$. Thus in the fractional regime the effective Luttinger parameter should be greater than 1 and no zero-bias peak should be seen in this regime.

For values of the Luttinger parameter $K < 1/2$ the tunneling conductance G_t , shown in Fig. 3 for $K=1/3$ and $K=1/5$, becomes negative for sufficiently large values of eV/T_K . To understand this interesting feature we recall that the expression of the tunneling current for $eV/T_K > e^\delta$ can be obtained from the second line of Eq. (3.12) in the form

$$I_t(V) = \frac{e^2 V}{h} K \sum_{n=1}^{\infty} a_n(K) \left(\frac{eV}{T_K} \right)^{2n(K-1)}, \quad (3.14)$$

with the coefficients a_n given by

$$a_n(K) = \frac{1}{1/2 + n(K-1)} c_n(K). \quad (3.15)$$

Since the tunneling coupling should make the tunneling current increase, one expects $a_1 > 0$ which implies $c_1(K) < 0$ for $K < 1/2$ from the above relation between a_n and c_n . This negative value of c_1 for $K < 1/2$ causes the conductance to become negative at large voltages and produces a dip in the conductance curve for $K=1/3$ and $K=1/5$ in Fig. 3. This phenomenon has same origin as the conductance along the quantum wire becoming larger than Ke^2/h in Ref. 22 and Koutouza, Siano, and Saleur reported similar phenomena in their work where they considered the charging effect on the tunneling between quantum wires.³² However, the negative conductance is expected only for practically infinite driving voltage at zero temperature since T_K is infinitely large at the strong-coupling fixed point and a numerical calculation of the TBA shows that this effect disappears for small V/T .²²

Now let us turn to the finite-temperature case. In contrast to the zero-temperature behavior of indefinite running, the effective tunneling coupling Γ stops running at a certain value $\Gamma^*(T)$ determined by the temperature at finite temperature. As in all quantum phase transitions,³³ this effect in turn leads to the appearance of a finite temperature-

dependent crossover scale $T_K^*(\Gamma^*(T), K)$. Furthermore, now both temperature and external voltage act as natural crossover energy scales. From the point of view of our scenario, finite temperature plays important role in understanding the peculiar features of the experiment, which can be summarized as follows.

- (1) Existence of a region in the filling factor with the ZBC peak.
- (2) Substantially low height of the conductance peak as compared to typical Hall conductance $\nu e^2/h$.
- (3) Appreciably large width of the peak region beginning at $\nu^* \sim 1$.
- (4) Disappearance of the ZBC peak as ν is increased beyond $\nu \sim 1$.
- (5) Reappearance of the ZBC peak in a region near and above $\nu \sim 2$.

It turns out that, except for the reappearance of the zero-bias peak near $\nu=2$, most of these effects can be understood within the point-contact scenario that we advocate here provided thermal crossover effects are taken into account. The reappearance of the peak near $\nu \sim 2$ will be discussed in the next section. The rest of this section will be devoted to our understanding on the first four aspects.

A central feature of this problem is the powerful fact that the differential tunneling conductance G_t is a universal scaling function of two dimensionless ratios T/T_K and V/T . First of all, the system behaves qualitatively as if it were at $T=0$ as long as the temperature is the smallest among three energy scales, i.e., $T \ll T_K, V$. In this regime the system flows to the stable fixed point at $\Gamma \rightarrow \infty$ where the tunneling current is large and the conductance saturates to its largest value Ke^2/h at ZBC. However, since the crossover scale T_K is a (weak) function of ν , there exists a filling factor ν^* for which $T_K(\nu^*) = T_K^* \sim T$. For $T > T_K^*$ the system will flow toward the decoupled unstable fixed point at $\Gamma=0$. Hence, in contrast with the case $T=0$ we expect only a crossover, instead of a phase transition. In particular this also means that, at low but fixed temperature T , we should see an appreciable increase in G_t when V becomes smaller than T_K^* , since T_K^* will be finite at nonzero temperature. However, as V becomes comparable to T the system will begin to be driven by thermal fluctuations, and the coupling Γ would no longer increase further as the voltage is lowered, thus leading to a saturation of the tunneling conductance at a value determined by temperature. Therefore, even though the ZBC peak should be observable due to an increase in G_t as the voltage is lowered past T_K^* , the height of the peak (essentially determined by the temperature) would be much lower than the zero-temperature saturation value Ke^2/h . Conversely, if the temperature is higher than T_K , thermal fluctuations dominate for all values of V and no ZBC peak should be observed.

On the other hand, in the regime where the filling factor is such that $K < 1$, the dependence of T_K on the tunneling amplitude Γ is such [see Eq. (3.10)] that as the filling factor ν increases, the exponent in the dependence of T_K upon Γ decreases. Hence, as ν is increased well past a value $\nu \sim 1$, the crossover scale T_K decreases, and at some point it becomes lower than the temperature. In this regime the junc-

tion is effectively in the high-temperature regime and the ZBC peak is absent. Thus, in the point-contact scenario, the gradual but rapid disappearance of the ZBC peak is a manifestation of this crossover.

This discussion can be made more explicit by looking at the behavior of the β function defined as

$$\beta(\Gamma, V, T) \equiv -\frac{\partial \Gamma}{\partial \ln V}. \quad (3.16)$$

This renormalization group function measures the change of the effective coupling constant Γ at temperature T as the external voltage V is varied. The statement that the conductance is a scaling function of the ratios T/T_K and V/T is equivalent to saying that one can define a set of systems which have the same conductance as the external voltage is varied. This set of equivalent systems amounts to a renormalization group flow defined by the Callan-Symanzik equation

$$\frac{dG_t}{d \ln V}(T/T_K, V/T) = \frac{\partial G_t}{\partial \ln V} + \frac{\partial \Gamma}{\partial \ln V} \frac{\partial G_t}{\partial \Gamma} = 0, \quad (3.17)$$

where the second term on the right-hand side of the first equality comes from the fact that T_K has an intrinsic dependence upon the coupling constant Γ . Note that in Eq. (3.17) we chose to vary the energy scale V instead of the cutoff scale, which as usual is hidden in the definition of T_K . This equation can be used to calculate the β -function defined in Eq. (3.16):

$$\beta(\Gamma, V, T) = \frac{\frac{\partial G_t}{\partial \ln V}}{\frac{\partial G_t}{\partial \Gamma}} = \frac{V \frac{\partial G_t}{\partial V}}{\frac{1}{1-K} \frac{T_K}{\Gamma} \frac{\partial G_t}{\partial T_K}}, \quad (3.18)$$

where we used the relation between T_K and Γ , Eq. (3.10), for the second equality.

As we shall see below, looking at the properties of this β function is a useful way to understand the temperature and voltage dependence of the differential tunneling conductance, and in particular it provides a simple intuitive way to describe the crossovers. However, we should alert the reader that this ‘‘phenomenologically defined’’ β function does not necessarily coincide with the standard definition of the renormalization group (RG) β function which is obtained by the flow in coupling constant space induced by integrating out a finite number of high-energy degrees of freedom. The standard RG β function is by definition an analytic function of the parameters. By scaling, $\beta(\Gamma, V, T)$ of Eq. (3.18) is a dimensionless function of the dimensionless ratios T/T_K and V/T , where T_K encodes all dependence on the microscopic coupling constant Γ . We will see below that this β function is analytic everywhere except at $(V, T) = (0, 0)$, since the limits $V \rightarrow 0$ and $T \rightarrow 0$ do not commute.

At zero temperature, using Eq. (3.12) it is easy to see that $V \partial G_t / \partial V = -T_K \partial G_t / \partial T_K$, and we obtain the expected result³¹

$$\beta(\Gamma, V, T=0) = -(1-K)\Gamma. \quad (3.19)$$

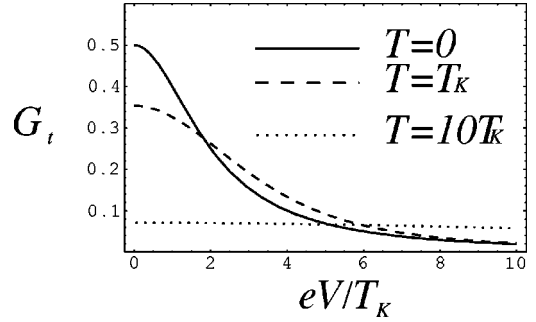


FIG. 4. The exact differential tunneling conductance given by Eq. (3.20) is plotted as a function of eV/T_K for different values of T/T_K for $K=1/2$. Observe the lowering and broadening of the peak as the temperature is increased.

In order to analyze the β function at finite temperature, we now turn to the $K=1/2$ case in which an exact G_t is known in closed form even at finite temperature, by refermionizing the even boson theory to a noninteracting spinless free fermion. In this special case, not only the conductance, but all n -point correlation functions are exactly solvable^{4,22,34} and the integral in the Eq. (5.2) of Ref. 22 can be reexpressed in terms of the digamma function $\psi(x) = \Gamma'(x)/\Gamma(x)$, leading to the expression for the conductance,

$$G_t(T, V, K=1/2) = \frac{1}{2} \frac{e^2}{h} \frac{T_K}{\pi T} \text{Re} \psi' \left[\frac{1}{2} + \frac{T_K}{\pi T} + \frac{ieV}{2\pi T} \right]. \quad (3.20)$$

The plot of $G_t(T, V, K=1/2)$ as a function of eV/T_K for several values of T/T_K in Fig. 4 shows the broadening of the peak as the temperature is increased. The reduction and eventual disappearance of the peak height at high temperatures is quite obvious in the plot of the ZBC peak height as a function of T/T_K in Fig. 5. One can also understand the gradual disappearance of the ZBC peak as ν is further increased as following. From Eqs. (3.10) and (2.9), we see that T_K decreases as ν increases for $K < 1$. Therefore, as ν becomes larger at given T , G_t will be determined by lower T_K , leading to a smaller ZBC peak which would eventually disappear.

The role of temperature on the peak height can also be seen by looking at the asymptotic behavior of $G_t(T, V=0, K=1/2)$ in the limit of $T \rightarrow 0$. At $V=0$,

$$G_t = \frac{1}{2} \frac{e^2}{h} \frac{T_K}{\pi T} \psi' \left(\frac{1}{2} + \frac{T_K}{\pi T} \right) \quad (3.21)$$

from Eq. (3.20). In the limit $T \rightarrow 0$, we can use the asymptotic expansion of the digamma function,

$$\psi(x) \sim \ln x - \frac{1}{2x} + \dots, \quad \text{for } |x| \gg 1, \quad (3.22)$$

to infer the asymptotic behavior of the peak height in the low temperature limit as

$$G_t \sim \frac{1}{2} \frac{e^2}{h} \left[1 - \frac{1}{4} \left(\frac{\pi T}{T_K} \right)^2 - \dots \right], \quad (3.23)$$

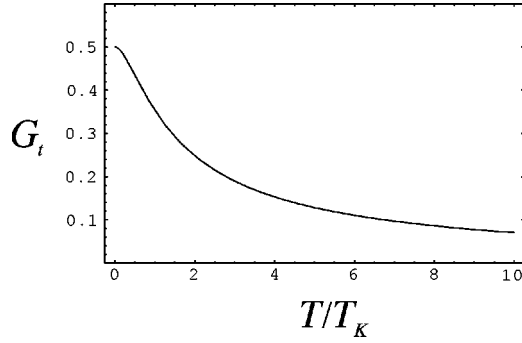


FIG. 5. The zero-bias conductance peak height $G_i(T, V=0, K=1/2)$ is plotted as a function of temperature.

where the decrease of the peak height at finite temperature is evident.

Although it is possible to calculate the differential conductance at zero bias for more general values of the Luttinger parameter K , it involves solving a set of complex coupled integral equations. This has been done numerically for the related problem of tunneling into a Luttinger liquid in the work of Koutouza, Siano, and Saleur³² who find that the results vary quite smoothly as K changes below $1/2$. (The main differences arise due to an analog of the “resonance” found earlier by Fendley, Ludwig, and Saleur.²² This resonance is responsible for the negative differential conductance at large voltages and at $T=0$.) Thus, at least at a qualitative level, it seems that the behavior for K below $1/2$ can be described by a curve like that of Eq. (3.20), for some crossover scale T_K , but with K replacing the overall factor of $1/2$. Preliminary results indicate that this is also a quantitatively accurate description of the data.²⁰

With the full expression for the conductance, Eq. (3.20), we can calculate the β function, Eq. (3.18), to obtain

$$\beta(\Gamma, V, T) = -\frac{1}{2}\Gamma \frac{eV}{2\pi T} \frac{\text{Im} \psi^{(2)}(z)}{\text{Re} \psi^{(1)}(z) + \frac{T_K}{\pi T} \text{Re} \psi^{(2)}(z)}, \quad (3.24)$$

where $z = 1/2 + T_K/\pi T + ieV/2\pi T$ and $\psi^{(n)}(z)$ stands for the n th derivative of the digamma function. This result is shown in Fig. 6 in the form of the plot of $\beta(V, T)/\beta(V, T=0)$ as a function of T/T_K and eV/T_K . From the above expression, we can immediately read off that

$$\lim_{V \rightarrow 0} \beta(\Gamma, V, T \neq 0) = 0, \quad (3.25)$$

which means that the coupling stops running at $V=0$ at finite temperature. Comparing Eq. (3.25) to Eq. (3.19) which gives $\beta(\Gamma, V, T=0) = -\Gamma/2$ for the case of consideration $K=1/2$, we can see that the limits $T \rightarrow 0$ and $V \rightarrow 0$ do not commute. Hence, we conclude that there is a singularity at $T=V=0$, simply illustrating the fact that the coupling runs indefinitely only at zero temperature due to the underlying quantum phase transition at $K=1$. This implies that all we should be able to see at any finite temperature is a crossover from $T > T_K$ to $T < T_K$ near $K \sim K^* < 1$ at which the tunneling in-

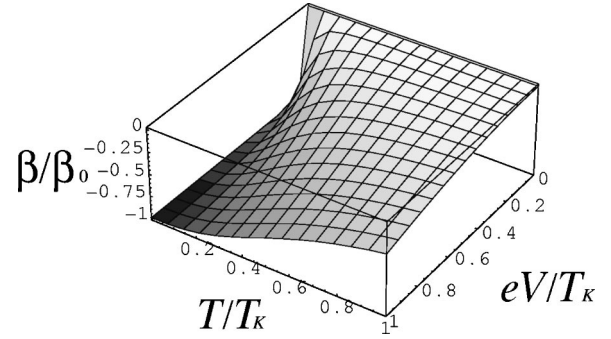


FIG. 6. The exact β function in units of $\beta_0 \equiv \beta(V, T=0) = \Gamma/2$ is shown as a function of eV/T_K and T/T_K . There is a crossover between the $T \rightarrow 0, V \neq 0$ limit, where $\beta \rightarrow -1/2\Gamma$, and the $V \rightarrow 0, T \neq 0$ limit, where $\beta \rightarrow 0$ near $T \sim V$: as the temperature is increased past V , the β function approaches zero where the coupling stops to run. This crossover explains the low height of the peak, which eventually disappears as ν is increased well beyond 1, leading to a smaller T_K .

creases rapidly as K becomes smaller than K^* , giving rise to a pronounced ZBC peak as ν is increased past $\nu^* > \nu_c$. This explains why the experiment sees a rapid increase of the ZBC peak when ν is increased past $\nu^* \geq 1$, even though we expect $\nu_c < 1$ due to the effects of the Coulomb interaction. Furthermore, since the behavior of the β function is quite different for $V=0$ and $T=0$, we expect a crossover near $V \sim T$, which was discussed earlier in relation to the existence of a peak region with finite width and the low height of the peak in the region. These crossover effects and the behavior of the β function are shown in Fig. 6. This result illustrates our general statement that it is the competition between the temperature and bias voltage that enables us to observe the conductance peak, and the height of the peak can be much lower than the saturation value Ke^2/h since the observable height will be limited by the temperature. This result also supports our argument that competition between T and T_K eventually leads to the disappearance of the peak as the filling factor is raised further past a value $\nu \sim 1$.

In this section, we gave a detailed analysis of the experimental predictions of our model, which was developed in the previous section. After mapping the problem to the BSG model, by borrowing known exact results of the BSG problem and calculating the relevant β function, we suggested consistent explanations to the so-far-not understood peculiar features of the experiment by Kang and co-workers. In our picture, finite-temperature effects are responsible for the observability of a ZBC peak with an unexpectedly low value of its height, as well as to the finite width in filling factors where the peak is observed.

Our picture is a natural consistent scenario for the appearance of the ZBC peak in the wide range of filling factor near $\nu \sim 1$. In the next section we will show that the reappearance of the ZBC peak in the range of filling factor near $\nu \sim 2$ in principle can also be understood by following closely the approach of this section for the $\nu \sim 1$ case but now considering the possibility of a partially spin-polarized state near $\nu \sim 2$.

IV. TUNNELING CONDUCTANCE NEAR AND ABOVE $\nu=2$

To understand the peak in the $\nu \sim 2$ region, we first note that this peak region begins abruptly near $\nu \sim 2$ in an apparently similar manner as it does near $\nu \sim 1$.¹² In the bulk system, as the filling factor becomes comparable to $\nu \sim 2$, the electron spin begins to matter, as the spin-reversed states begin to get progressively occupied. Thus, even if the 2DEG is fully polarized for $\nu \sim 1$, spin plays a crucial role for $\nu \sim 2$. In addition, for samples with high nominal electronic density, spin fluctuations are known to become important and in some cases so much that the ground state may even be a spin singlet. However, this situation requires samples with fairly high densities, which is presumably not the case in the experiment of Kang and co-workers. Hence, a natural extension of the picture that we advocated for in the previous section, as it stands applicable only for fully polarized 2DEG's, simply requires us to take into account the changes in the physics brought about by the electron spin and, in particular, of the role played by both Zeeman and exchange interactions. This extension should be applicable to both spin-singlet and -nonsinglet cases. However, once the spin degrees of freedom is included, there is a richer class of possible behaviors, for there are now three possible types of tunneling corresponding to tunneling of charge and/or spin degree of freedom. In what follows we will be interested mostly in the regime in which the spin polarization is not large. Hence, we will assume a reference state in which the up- and down-spin branches have the same filling factor $\nu_\uparrow = \nu_\downarrow$ and investigate the effects of the Zeeman term which will tend to polarize the state. We will focus on states with total filling factor $\nu \geq 1$. For these states the outermost edge is a $\nu = 1$ edge (per spin component). Effects of the magnetic field thus enter in the choice of the range of filling factor $\nu \geq 2$, in the presence of spin exchange interactions, and in effects of the Zeeman term as well as other possible SU(2) symmetry breaking terms on the edge states. We will consider two different physical situations: (1) when the SU(2) symmetry of the spin is broken either by a (large) Zeeman term, in which case the ground state may be polarized (although not necessarily fully polarized), or by magnetic anisotropy terms (expected to be very small in these systems), and (2) when the Zeeman term is small enough that the ground state is a singlet at $\nu = 2$. There are a number of other interesting cases, such as the singlet and partially polarized states at $\nu < 2$, which will not be discussed here. These states have interesting tunneling properties³⁵ but do not exhibit the ZBC peak in the tunneling conductance that we are discussing here.

The Hamiltonian density that was studied in the previous section can be easily modified to account for the spin degree of freedom and its interactions. Thus, we write the Hamiltonian density in terms of the spin-dependent chiral electron densities $J_{\pm, \alpha} \equiv \psi_{\pm, \alpha}^\dagger \psi_{\pm, \alpha}$, with spin projection $\alpha = \uparrow, \downarrow$. Furthermore, the spin-spin exchange interaction and Zeeman term should now be included in the Hamiltonian density. Let us define the charge densities operators of chiral modes as $J_{\pm}^c \equiv J_{\pm, \uparrow} + J_{\pm, \downarrow}$ and the three-component spin densities op-

erator $J_{\pm}^a \equiv \frac{1}{2} \psi_{\pm, \alpha}^\dagger \sigma_{\alpha\beta}^a \psi_{\pm, \beta}$, where σ^a are Pauli matrices, with $a = x, y, z$. The Hamiltonian density for the system of two coupled edges can be written as a sum of charge and spin Hamiltonians,

$$\mathcal{H}_G = \mathcal{H}_c + \mathcal{H}_s. \quad (4.1)$$

The charge Hamiltonian is given by

$$\mathcal{H}_c = \frac{\pi v_c}{2} (J_+^c J_+^c + J_-^c J_-^c + 2g_c J_+^c J_-^c), \quad (4.2)$$

where both the bare edge velocity and the effects of the intraedge interactions are absorbed in the effective charge velocity v_c . We will write the spin part of the Hamiltonian as a sum of two terms,

$$\mathcal{H}_s = \mathcal{H}_{\text{symm}} + \mathcal{H}_{\text{pert}}, \quad (4.3)$$

where the SU(2)-invariant part has the form³⁶

$$\mathcal{H}_{\text{symm}} = \frac{2\pi}{3} v_s (\vec{J}_+ \cdot \vec{J}_+ + \vec{J}_- \cdot \vec{J}_- + 6g_s \vec{J}_+ \cdot \vec{J}_-). \quad (4.4)$$

Here v_s includes the effects of intraedge spin interactions and g_s is the interedge strength of the exchange interaction.

We have used a simple and rather crude model to estimate the interedge exchange coupling constant. We modeled the barrier with a potential $V(x)$ of height V_0 and width $2a$. We find that, as expected, due to the antisymmetry of the wave function, the dimensionless coupling constant g_s has a ferromagnetic sign and that its magnitude has a rapid dependence of $k_F \ell$ where k_F is the Fermi wave vector of the edge states. For a barrier of width 88 Å and height 220 meV, and for a model in which correlations enter only in the antisymmetry of the wave function, we estimate that reasonable values of the dimensionless interedge exchange coupling constant are quite small, typically in the range $|g_s| \sim 10^{-3} - 10^{-4}$. While it is quite possible that we are underestimating the magnitude of g_s , it seems unlikely that a realistic value can be larger by more than an order of magnitude. In addition, we show below that for the ferromagnetic sign, interedge exchange interactions are (marginally) irrelevant. Hence it is reasonable to set g_s to zero if $g_s < 0$, since the expected (logarithmic) corrections to scaling will be exceedingly small.

The Hamiltonian for the symmetry breaking perturbations, i.e., a Zeeman term and an anisotropy term, is

$$\mathcal{H}_{\text{pert}} = -\mu_B g B (J_+^z + J_-^z) + 4\pi v_s g_s \lambda J_+^z J_-^z, \quad (4.5)$$

where μ_B is the Bohr magneton, g is the gyromagnetic ratio, and λ measures the strength of the magnetic anisotropy (which is quiet likely to be very small in the samples of Kang and co-workers). For $\lambda > 0$ the anisotropy is Ising like and for $\lambda < 0$ it is XY like. For notational convenience, we define the XY component exchange coupling g_\perp and Ising exchange coupling g_\parallel :

$$g_\perp \equiv g_s, \quad g_\parallel \equiv (1 + \lambda) g_s. \quad (4.6)$$

Experimentally it is known that in GaAs the gyromagnetic factor is anisotropic and that this anisotropy is quite large for

the geometry of the experiment of Kang and co-workers.³⁷ The magnitude (and sign) of the magnetic anisotropy (anisotropy in the exchange interaction) are apparently not known. As we will see below the magnetic anisotropy can potentially lead to interesting effects such as a possible spin-gap state. However, given the smallness of our estimate of the exchange interaction we should expect the spin gap to be small as well. Nevertheless, in spite of the possible small value of this gap, we will discuss the interesting physics of this state.

We will treat the spin-1/2 case using Abelian bosonization, much in the way we did the spin-polarized case in the previous section. However, we will pay special attention to the role of the SU(2) spin symmetry which is not manifest in Abelian bosonization. In any event we will also be interested in situations in which the SU(2) symmetry is explicitly broken (say, by the Zeeman term) and in that case Abelian bosonization is the most direct way to solve this problem. Hence we proceed to use the standard Abelian bosonization approach in a similar manner as in Sec. II except that now the chiral Fermi fields are spin dependent.

The right- and left-moving chiral Fermi fields with spin $\alpha = \uparrow, \downarrow$ are bosonized according to the Mandelstam formula

$$\psi_{\pm\alpha}^{\dagger} = \frac{1}{\sqrt{2\pi}} e^{\pm i\phi_{\pm,\alpha}(x)}, \quad (4.7)$$

where $\phi_{\pm,\alpha}$ are spin-dependent chiral right- and left-moving Bose fields, respectively. The corresponding bosonized normal-ordered density operators are

$$J_{\pm,\alpha} = -\frac{1}{2\pi} \partial_x \phi_{\pm,\alpha}. \quad (4.8)$$

Extending the expression in Eq. (2.5) to the partially spin-polarized case of concern, the Lagrangians for each spin component of the decoupled noninteracting edges are

$$\mathcal{L}_{\pm,\alpha}[\phi_{\pm,\alpha}] = \frac{1}{4\pi} \partial_x \phi_{\pm,\alpha} (\pm \partial_t - v_0 \partial_x) \phi_{\pm,\alpha}. \quad (4.9)$$

The chiral boson fields $\phi_{\pm,\alpha}$ can be decomposed into their spin and charge components:

$$\phi_{\pm,c} = \frac{1}{\sqrt{2}} (\phi_{\pm,\uparrow} + \phi_{\pm,\downarrow}), \quad \phi_{\pm,s} = \frac{1}{\sqrt{2}} (\phi_{\pm,\uparrow} - \phi_{\pm,\downarrow}). \quad (4.10)$$

In terms of these chiral charge and spin bosons, the right-moving electron operators are (up to Klein factors)

$$\psi_{\pm,\uparrow/\downarrow}^{\dagger} \sim \frac{1}{\sqrt{2\pi}} e^{(i/\sqrt{2})\phi_{c,+}} e^{\pm(i/\sqrt{2})\phi_{s,+}}; \quad (4.11)$$

i.e., the electron splits into a spin-1/2 charge-neutral spinon and a charge-1 spin-0 holon.

The chiral charge currents $J_{c,\pm}$ are

$$J_{c,\pm} = -\frac{\sqrt{2}}{2\pi} \partial_x \phi_{c,\pm}. \quad (4.12)$$

The coefficient $\sqrt{2}$ in front of the charge current shows that the filling factor is $\nu=2$. In what follows, exactly as what we found for fully polarized states, changes in the filling factor will only appear through the dependence on ν of the coupling constants. However, the coefficient of the current will remain unchanged.

The corresponding expressions for the chiral spin currents $J_{a,\pm}$, $a=x,y,z$, the three generators of the $su(2)_1$ Kac-Moody algebra of spin, are

$$\begin{aligned} J_{x,\pm} &= \frac{1}{2\pi} \cos(\sqrt{2}\phi_{s,\pm}), \\ J_{y,\pm} &= \pm \frac{1}{2\pi} \sin(\sqrt{2}\phi_{s,\pm}), \\ J_{z,\pm} &= -\frac{1}{2\pi} \frac{1}{\sqrt{2}} \partial_x \phi_{s,\pm}. \end{aligned} \quad (4.13)$$

The factors of $\sqrt{2}$ are crucial for the system to be invariant under the SU(2) symmetry of spin.³⁸

In the absence of electron tunneling at the point contact, the Hamiltonian for the line junction reduces to $\mathcal{H} = \mathcal{H}_c + \mathcal{H}_s$ of Eq. (4.2) and Eq. (4.3), respectively. Thus we recover the familiar spin-charge separation of one-dimensional interacting electronic systems. This Hamiltonian has been studied extensively in the literature (see, for instance, the pedagogical discussion in Ref. 36). The charge sector \mathcal{H}_c behaves exactly as in the spin-polarized case of Sec. II. The only difference here is the factor of $\sqrt{2}$ in the definition of the (bosonized) chiral charge currents which reflect the fact that these are the edge states of two quantum Hall states each with filling factor $\nu=2$. Thus the discussion of Sec. II implies that the charge sector is described by a rescaled charge boson $\varphi_c = (\phi_{c,+} + \phi_{c,-})/\sqrt{K_c}$, with Lagrangian

$$\mathcal{L}_c = \frac{1}{8\pi} \left(\frac{1}{v_c} (\partial_t \varphi_c)^2 - v_c (\partial_x \varphi_c)^2 \right), \quad (4.14)$$

with a charge Luttinger parameter K_c equal to

$$K_c = \sqrt{\frac{1-g_c}{1+g_c}}. \quad (4.15)$$

Note that $K_c < 1$ since $g_c > 0$. The compactification radius of the charge boson φ_c is $R_c = \sqrt{2/K_c}$. The velocity of the charge boson is renormalized exactly as in the spin-polarized case, i.e., $v_c = v_0 \sqrt{1-g_c^2}$.

Naturally, the main difference between the case with a small spin polarization and the fully polarized case resides in the spin sector with effective Hamiltonian \mathcal{H}_s . The first two terms of the SU(2)-symmetric part of spin Hamiltonian of Eq. (4.4) represent two decoupled edges with exact SU(2) symmetry. In fact, this is a fixed-point Hamiltonian of two chiral $su(2)_1$ Wess-Zumino-Witten conformal field theories. Except for the renormalization of the velocities, due to forward-scattering intraedge interactions, this is a free

theory. In Abelian bosonization the first two terms of the Hamiltonian of Eq. (4.4), which we will denote by $\mathcal{H}_{s,\pm}$, are given by³⁸

$$\mathcal{H}_{s,\pm} = \frac{2\pi}{3} v_s \vec{J}_{s,\pm}^2 = \frac{v_s}{4\pi} (\partial_x \phi_{s,\pm})^2. \quad (4.16)$$

The interedge exchange interaction term, with coupling constant g_s , is a chirality breaking perturbation and its effects are well known.³⁶ After Abelian bosonization, the Ising component exchange interaction only renormalizes the velocity and the compactification radius of the spin boson but the XY component exchange introduces a cosine term as can be seen in the bosonized effective Lagrangian

$$\begin{aligned} \mathcal{L}_s = & \frac{1}{8\pi} \left(\frac{1}{v'_s} (\partial_t \varphi_s)^2 - v'_s (\partial_x \varphi_s)^2 \right) - \frac{v_s g_\perp}{\pi} \cos(\sqrt{2K_s} \varphi_s) \\ & - \frac{\mu_B g B}{\pi} \sqrt{\frac{K_s}{2}} \partial_x \varphi_s, \end{aligned} \quad (4.17)$$

where g_\perp and g_\parallel are defined in Eq. (4.6) and the last term is the Zeeman term. In Eq. (4.17), φ_s is the rescaled spin boson,

$$\varphi_s = (\phi_{s,+} + \phi_{s,-}) / \sqrt{K_s}, \quad (4.18)$$

with the Luttinger parameter K_s , the renormalized velocity v'_s , and the compactification radius of the spin boson given by

$$K_s = \sqrt{\frac{1-g_\parallel}{1+g_\parallel}}, \quad v'_s = v_s \sqrt{1-g_\parallel^2}, \quad R_s = \sqrt{2/K_s}. \quad (4.19)$$

A. Small Zeeman term

Let us discuss first the case when the Zeeman energy is very small. Although this case does not apply to the samples used in the experiments of Ref. 12, in which the Zeeman interaction is not small, nevertheless it is a good starting point for a theoretical analysis of this problem. The renormalization group (RG) β functions for the exchange interaction coupling constants are well known to have the form^{24,39,40}

$$\begin{aligned} \frac{dg_\perp}{d \ln a} &= 2g_\perp g_\parallel - 5g_\perp^3 + \dots, \\ \frac{dg_\parallel}{d \ln a} &= 2g_\perp^2 + 4g_\perp^2 g_\parallel + \dots, \end{aligned} \quad (4.20)$$

where a is a length scale. The resulting RG flow is sketched in Fig. 7. The consequence of the flow depends on the anisotropy of the interaction and the sign of the coupling as the following.

1. SU(2)-symmetric case

This model describes two $\nu=2$ *singlet* quantum Hall states coupled along a line junction. In this case we can define a single coupling constant $g_s \equiv g_\perp = g_\parallel$. In spite of the

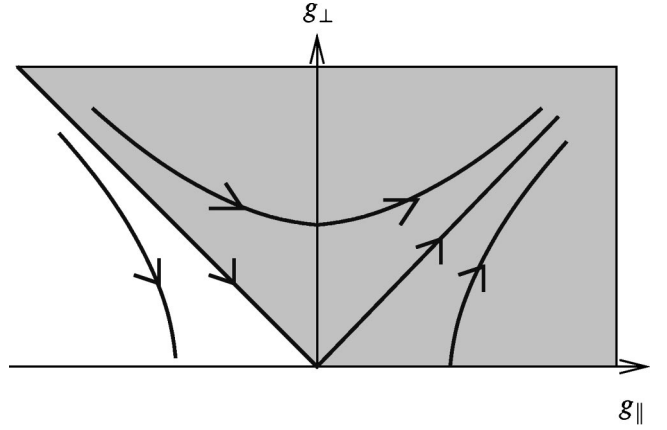


FIG. 7. The RG flow of Eq. (4.20). The trajectories starting at points in the shaded region flow to the spin-gap phase.

anisotropic look of Eq. (4.17), the relation between K_s and g_\perp , which is same as g_\parallel in this case, guarantees that the allowed RG flows are SU(2) invariant.

From Eq. (4.20), the RG β function for g_s is

$$\beta(g_s) = \frac{dg_s}{d \ln a} = 2g_s^2 - 2g_s^3 + \dots. \quad (4.21)$$

For $g_s < 0$, i.e., *ferromagnetic* exchange coupling, the cosine term is a *marginally irrelevant* perturbation. Hence in the low-energy regime the effective coupling vanishes, $g_s \rightarrow 0$, albeit very slowly, giving rise to logarithmic corrections to scaling. Thus, for $g_s < 0$ the spin sector of the line junction remains gapless and $K_s \rightarrow 1$, $R_s \rightarrow \sqrt{2}$, a result originally found by Luther and Emery⁴¹ in the theory of the one-dimensional electron gas. This is presumably the relevant case for the line junction in the SU(2)-symmetric regime since the interedge exchange interaction is naturally ferromagnetic. However, we will see below that magnetic anisotropy can make the antiferromagnetic regime accessible.

In contrast, for $g_s > 0$, i.e., *antiferromagnetic* exchange coupling, this perturbation is *marginally relevant* and the flow is asymptotically free. In this case the effective coupling constant g_s flows to large values where scale invariance is violated. Hence, in this case the system flows to a phase with an energy gap in the spin sector, a *spin-gap state*, along the SU(2)-invariant RG trajectory. This state is physically equivalent to the Haldane phase⁴² of one-dimensional quantum Heisenberg antiferromagnets and to the Luther-Emery liquid of the one-dimensional electron gas.⁴¹ In particular, for $K_s = 1/2$, the spin boson φ_s is equivalent to a massive fermion. This is the well-known Luther-Emery point.

For small values of the coupling constant g_s the magnitude of the spin gap Δ_s can be determined by perturbative renormalization group methods. For a strictly SU(2)-invariant system the spin gap is the well-known result

$$\Delta_s(g_s) = D \sqrt{g_s} e^{-1/2g_s}, \quad (4.22)$$

where D is an ultraviolet cutoff of the order of a fraction of the Fermi energy. (The factor of $\sqrt{g_s}$ is due to corrections to scaling which appear at two-loop order in g_s .) Given the apparent smallness of the exchange coupling constant g_s ,

this result is probably good enough here. For larger values of g_s the spin gap can be determined either from the full Bethe-ansatz solutions of the sine-Gordon and chiral Gross-Neveu models or at special points, such as the Luther-Emery point, from bosonization arguments. In both cases in addition to the spin gap one finds a spectrum of solitons which should lead to interesting resonance effects in tunneling.

2. Effects of a small magnetic anisotropy

Let us now discuss what happens if there is a small magnetic anisotropy, i.e., a small anisotropy in the exchange interaction. Presumably for the samples used in the experiments of Kang and co-workers,¹² if there is any anisotropy at all, it is exceedingly small. However, we will discuss this case here since it leads to interesting effects. Magnetic anisotropy makes the Ising exchange coupling g_{\parallel} differ from the XY exchange g_{\perp} . In this case the RG flow no longer follows the SU(2)-invariant trajectory. It is easy to see from the β functions, Eq. (4.20), that for $g_s > 0$ (in which case both g_{\parallel} and g_{\perp} are positive), the line junction will flow toward the spin-gap state.

However, for $g_s < 0$, the RG flows depend on the anisotropy. With Ising-like anisotropy ($\lambda > 0$) and $g_s < 0$, the RG trajectories flow toward the line of fixed points at zero sine-Gordon coupling constant and $K_s > 1$. Conversely with XY-like anisotropy ($\lambda < 0$) we get the opposite result. In this case, the RG trajectories still flow initially toward the free theory ($g_{\perp} \rightarrow 0$). However, they will eventually be driven to the marginally relevant flow of the SU(2) trajectory, leaving the $su(2)_1$ fixed point. Hence, in this regime the line junction flows toward the spin-gap state. Thus, even though the initial value of the interedge interaction is negative, $g_s < 0$, an arbitrarily small XY anisotropy drives the line junction necessarily to a spin-gap state. This is a remarkable effect which leads us to conclude that there is a phase transition at $\lambda = 0$. The discussion above is summarized in Fig. 7 where the region in the coupling constant space which flows to the spin-gap phase is shaded.

B. Effect of Zeeman interactions

Let us finally discuss the case of large Zeeman interactions. Physically this is the most important case. It is also the simplest. The charge sector is not affected by the Zeeman interaction, and it behaves exactly in the same way as in the previous cases. The effect of the Zeeman term on the spin sector depends on which regime the line junction is in. In the absence of a spin gap, which as we saw above happens for $g_s < 0$ in the SU(2)-symmetric case or with Ising-like magnetic anisotropy, the cosine term is irrelevant. In this case, the Zeeman term can be eliminated from the Lagrangian density by a shift of the spin field: $\varphi_s \rightarrow \varphi_s + 2\pi\gamma x/v_s$, where

$$\gamma \equiv \frac{\mu_B g B}{\pi} \sqrt{\frac{K_s}{2}}. \quad (4.23)$$

While this shift has no effect on the charge sector it forces a twist in the boundary conditions of the spin sector:

$$\Delta\varphi_s \equiv \int dx \partial_x \varphi_s \rightarrow \Delta\varphi_s + \frac{2\pi\gamma}{v_s} L, \quad (4.24)$$

where L is the length of the system (the barrier). Since $\partial_x \varphi_s$ is proportional to the spin density, the twist of BC's, Eq. (4.24), implies that the z component of the spin polarization, $M_z = \langle S_z \rangle$, is finite, $M_s \propto \gamma/v_s \propto BL$, and this state has a non-zero spin polarization, although in general is not fully polarized.

Hence, the only observable effect of the Zeeman term in the gapless phase is a nonzero spin polarization and hence a twist of the boundary conditions.

Let us now discuss the effects of the Zeeman term in the spin-gap phase. An examination of the effective Lagrangian \mathcal{L}_s of Eq. (4.17) shows that, as expected, there is competition between the Zeeman term and the cosine operator. This competition, which bears a close analogy with the mechanism of the commensurate-incommensurate transition, leads to different physical behaviors depending on which is the smallest energy scale, the Zeeman energy or the spin gap. When the Zeeman energy is small compared with the spin gap, the system will stay in the gapped phase despite the twist of BC's. However, when the Zeeman term dominates, the cosine operator once again becomes irrelevant and the spin gap is destroyed by the Zeeman interaction.

C. Tunneling transport

The discussions in the previous two subsections can be summarized as the following. Depending on the sign of the exchange interactions, magnetic anisotropy, and the strength of the Zeeman term, the spin sector of the system can be either in a spin-gap phase or a gapless phase. Let us finally look at the consequences of these results for the question of electron tunneling transport in the line junction. Due to the spin degree of freedom, there are now three possible types of tunneling corresponding to the tunneling of charge and/or spin degree of freedom. The lowest-order operators for each of these processes are the single-electron tunneling operator which transports both charge and spin,

$$\begin{aligned} \mathcal{O}_e &= \psi_{\uparrow,+}^{\dagger} \psi_{\uparrow,-} + \psi_{\downarrow,+}^{\dagger} \psi_{\downarrow,-} + \text{H.c.} \\ &\propto \cos\left(\sqrt{\frac{K_c}{2}}\varphi_c\right) \cos\left(\sqrt{\frac{K_s}{2}}\varphi_s\right), \end{aligned} \quad (4.25)$$

the spin-singlet pair (spin-0, charge-2) tunneling operator

$$\mathcal{O}_{pair} = \psi_{\uparrow,+}^{\dagger} \psi_{\downarrow,+}^{\dagger} \psi_{\downarrow,-} \psi_{\uparrow,-} + \text{H.c.} \propto \cos(\sqrt{2K_c}\varphi_c), \quad (4.26)$$

and the tunneling operator of a spin-1 charge-neutral excitation:

$$\mathcal{O}_s = \psi_{\downarrow,-}^{\dagger} \psi_{\downarrow,+} + \psi_{\uparrow,+}^{\dagger} \psi_{\uparrow,-} + \text{H.c.} \propto \cos(\sqrt{2K_s}\varphi_s). \quad (4.27)$$

The single-electron tunneling operator \mathcal{O}_e clearly mixes the charge and spin sectors. As far as the charge sector is concerned, this tunneling operator is similar to the one for fully polarized electrons shown in Eq. (2.10), except that instead

of the Luttinger parameter K we now have K_c , where K_c is the charge Luttinger parameter defined in Eq. (4.15). The spin sector has a similar structure with the effective Luttinger parameter K_s . The scaling dimension of the operator of Eq. (4.25) at a point contact is

$$d_e = \frac{1}{2}(K_c + K_s). \quad (4.28)$$

The singlet pair tunneling operator \mathcal{O}_{pair} which depends only on the charge boson and the holon pair tunneling operator \mathcal{O}_s which depends only on the spin boson are higher-order operators. At a point contact, \mathcal{O}_{pair} and \mathcal{O}_s have boundary scaling dimensions d_{pair} and d_s , respectively, given by

$$d_{pair} = 2K_c, \quad d_s = 2K_s. \quad (4.29)$$

Now let us discuss the possible effect of these operators in the spin-gap phase and the gapless phase. First, because the singlet pair tunneling operator \mathcal{O}_{pair} depends only on the charge boson, its effect is the same for the spin-gap phase and the gapless phase. Since the charge sector is free, the constraint of momentum conservation forbids singlet pair tunneling in the absence of a point contact. However, the operator \mathcal{O}_{pair} at a point contact is relevant for $K_c < 1/2$ in the presence of a strong Coulomb interaction [Eq. (4.29)] and it can lead to charge-only tunneling for both the spin-gap phase and gapless phases. On the other hand, the possibilities of the other two tunneling processes—namely, the single-electron tunneling and the holon-pair tunneling—depend on the presence or absence of the spin gap since their operator representation involves vertex operators of spin bosons.

1. Spin-gap phase

In the gapped phase, the spin boson field φ_s acquires an expectation value in the set $\varphi_s = 2n\pi/\sqrt{2K_s}$ where $n \in \mathbb{Z}$ which labels the manifold of degenerate ground states in the gapped phase. Since the value of $\cos(\sqrt{K_s}/2\varphi_s)$ alternates in this set, the expectation value of \mathcal{O}_e vanishes in this phase and the single-electron tunneling is (exponentially) suppressed in this regime. (This is a natural result since the electron carries spin 1/2.) Therefore, the lowest-order tunneling process that can contribute to a charge transport across the barrier is the singlet-pair tunneling, which is possible only through a point contact for both the spin-gap phase and gapless phase. Although this is a two-particle process, \mathcal{O}_{pair} can still lead to a ZBC peak even in this spin-gap phase if the Coulomb interaction is strong enough so that $K_c < 1/2$ which makes this operator relevant as we mentioned earlier. However, since \mathcal{O}_s is relevant and allowed everywhere along the barrier in the spin-gap phase (\mathcal{O}_s is the operator that causes the spin gap), there is a perfect spin tunneling in the absence of charge tunneling even in the absence of a point contact. The mechanism behind this effect in the spin sector is similar in spirit to the explanation of the ZBC peak in the charge tunneling conductance proposed by Mitra and Girvin.¹⁴ In fact this phase looks very much like a superconductor without phase coherence.⁴³

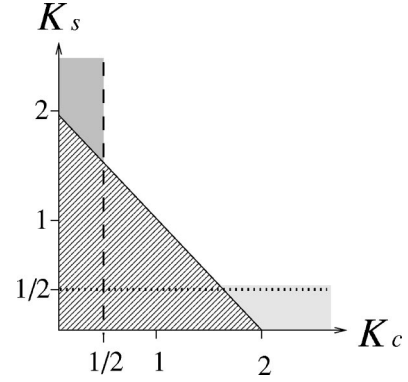


FIG. 8. The phase diagram near $\nu=2$. The peak in both the spin tunneling conductance and the charge tunneling conductance is expected in the crosshatched region below the line $K_c + K_s = 2$ where the single-particle tunneling operator is relevant. On the other hand, the charge-only tunneling operator \mathcal{O}_c and the spin-only tunneling operator \mathcal{O}_s , respectively, are relevant in the dark shaded region to the left of the dashed line and lightly shaded region below dotted line.

2. Gapless phase

In the gapless phase, \mathcal{O}_e or \mathcal{O}_s also are allowed only at a point contact and whether any of these operators are relevant or not depends on the Luttinger parameters. The effect of three tunneling operators \mathcal{O}_e , \mathcal{O}_{pair} , and \mathcal{O}_s at a point contact in the gapless phase is summarized in Fig. 8 as pointed out earlier by Kane and Fisher.⁴ The crosshatched region is where the single-particle tunneling operator \mathcal{O}_e is relevant and we expect the peak in both the spin tunneling conductance and the charge tunneling conductance. In the dark shaded region to the left of the dashed line, the charge-only tunneling operator \mathcal{O}_{pair} is relevant. Analogously, the spin-only tunneling operator \mathcal{O}_s is relevant in the lightly shaded region below the dotted line. Note that one has to keep in mind that $K_c < 1$ because of the Coulomb interaction.

For the SU(2)-symmetric gapless case (with ferromagnetic exchange) in which $K_s = 1$, the (boundary) scaling dimension of the electron tunneling operator is $(K_c + 1)/2 < 1$, since $K_c < 1$. Thus, the single-electron tunneling term is a relevant perturbation, and the coupling constant Γ flows to strong coupling in this case. Therefore, there should also be a zero-bias peak in the tunneling conductance in the case of a $\nu=2$ spin-singlet quantum Hall state, with qualitatively similar properties as the zero-bias tunneling peak for the spin-polarized case. With ferromagnetic exchange interactions and Ising-like anisotropy, in which case the system is in the gapless phase independent of the strength of the Zeeman term, $K_s > 1$, and Fig. 8 implies that holon-pair tunneling is always irrelevant in this case. However, if $1 < K_s < 2 - K_c$ for weak ferromagnetic interactions, the single-electron tunneling is relevant. Also with a strong enough Coulomb interaction, singlet-pair tunneling can become relevant. Finally, for a phase in which the gap is washed out due to a strong Zeeman term, $K_s < 1$, and again the single-electron tunneling is relevant.

To summarize, in both the spin-gap phase and gapless phase, there is no charge tunneling current in the absence of

a point contact. In the gapless phase, there underlies a quantum phase transition in the single-electron tunneling process through a point contact which leads to the reappearance of the zero-bias peak near $\nu \sim 2$ in a manner similar to the fully polarized case of the previous section. On the other hand, even though the single-electron tunneling is exponentially suppressed in the spin-gap phase, an analogous crossover in the singlet-pair tunneling channel can lead to the reappearance of the ZBC peak (in the regime of strong Coulomb interactions). This scenario is consistent with the experimental observation which displays a very close similarity between the manner in which the peak region appears abruptly and disappears gradually in both $\nu \sim 1$ and $\nu \sim 2$. Since the operator \mathcal{O}_e mixes the spin and charge sectors, in the regime in which this operator is relevant it induces a nonzero tunneling current of both charge and spin. Hence, if the observed ZBC peak near $\nu \sim 2$ is indeed caused by the single-particle tunneling operator in the phase without a spin gap, we expect that a *spin conductance* peak should be observable near $\nu \sim 2$ but not near $\nu \sim 1$, in marked contrast to charge conductance which would show a ZBC peak near both filling factors.

In this section, we extended the picture we advocated in the previous sections to the case of small spin polarization near $\nu \sim 2$ and investigated the changes in physics brought about by the electron spin. It was pointed out that the interplay between the Zeeman term and the exchange term enables us to identify two different phases in terms of their spin transport properties even in the absence of any point-contact operator: a spin-gap phase in which the spin excitations along the edge are gapped, and hence perfect spin tunneling, and a phase with gapless spin excitations. In both cases, there is no charge tunneling current in the absence of a point contact. Since in most cases of physical interest the edge states are likely to be in the gapless phase at least for a large enough Zeeman interaction, we proposed that here too there is a crossover in single-electron tunneling processes through a point contact, leading to the reappearance of the zero-bias peak near $\nu \sim 2$. In our picture, the apparent similarities in the patterns in which the peak region begins and disappears near two filling factors $\nu \sim 1$ and $\nu \sim 2$ in the experiment by Kang and co-workers can be understood in a natural and consistent way. The reappearance of the peak region near $\nu \sim 2$ had been totally unexplained in previous theories of tunneling between laterally coupled FQH states.^{14,16} We also discussed a number of interesting two-particle tunneling processes and the interesting behavior of spin tunneling in these systems.

V. CONCLUSIONS

In summary, in this paper we proposed a theoretical explanation of the questions raised by experiments of Kang and co-workers,¹² by modeling the system as a pair of coupled chiral Luttinger liquids with a point contact. Using standard bosonization methods we mapped the problem to the tunneling problem in Luttinger liquids first discussed by Kane and Fisher.^{4,5} Our results show that the interedge Coulomb interaction reduces the Luttinger parameter and moves the system

deep into the strong-coupling regime for $\nu \sim 1$, leading to the appearance of a zero-bias peak in the tunneling conductance with a peak value at $T=0$ of $G_t = Ke^2/h$, with $K < 1$. We mapped the problem onto integrable boundary sine-Gordon theory and used the known exact results of the BSG problem to obtain predictions for the behavior of the tunneling conductance. By considering a special solvable case, we determined the behavior of the conductance for all temperature and voltages. We investigated several crossovers of interest by introducing an appropriate β function. This analysis showed that the crossover between the $T=0$ behavior and the $V=0$ behavior yields a natural explanation of the low value of the “zero-bias conductance peak” measured in the experiment.¹² We also showed that the gradual disappearance of the peak as the filling factor is increased past $\nu \sim 1$ can be ascribed to the crossover between $T < T_K$ and $T > T_K$.

Furthermore, we considered the role of spin in this tunnel junction and showed that the reappearance of the ZBC peak in the region near the filling factor $\nu \sim 2$ can be understood if we assume that there is a (possibly small) spin polarization near $\nu \sim 2$. We extended the approach we used for fully polarized electrons with $\nu \sim 1$ to partially spin-polarized and unpolarized electrons with $\nu \sim 2$, by taking into account the role of Zeeman interactions, exchange interactions, and magnetic anisotropies. We discussed in detail the phase diagram of the system in this case and showed that the tunneling signature depends on whether the spin sector is gapped or not. We showed that the picture near $\nu \sim 1$ can be naturally extended to this new regime and that the single-particle tunneling operator can also give rise to a zero-bias tunneling conductance peak in both charge transport and spin transport in the gapless phase. Higher-order (multiparticle) point-contact operators can in principle lead to charge-only or spin-only tunneling, depending on the value of Luttinger parameters K_c and K_s . On the other hand, we found that spin transport along the edge is gapped even in the absence of a point contact when the Zeeman term is small and if there is a very weak *XY*-like magnetic anisotropy or if the exchange interaction is antiferromagnetic. In this regime we expect perfect tunneling of the spin current, which suggests future experimental tests of these ideas. Even though the single-electron tunneling is exponentially suppressed in the spin-gap phase, the singlet-pair tunneling can lead to a ZBC peak in the presence of a strong Coulomb interaction.

Our scenario is based on the assumption of a single tunneling center. When the bias voltage and the coupling between edge modes on each side of the barrier are weak enough to give a low peak in the tunneling conductance, as is observed in the experiment, the scenario of tunneling through a single tunneling center is quite likely to be an accurate description of the physics. Even though our picture is applicable only near (and above) $\nu = 1$ and $\nu = 2$, it offers a natural explanation of many salient features of the experiment which were not explained so far. This picture offers a consistent explanation for the reappearance of the ZBC peak and of the observed similarity in the manner in which the two peak regions near $\nu \sim 1$ and $\nu \sim 2$ appear and disappear. Our results also indicate that temperature should play an important role and that a temperature dependence of the data is

needed to understand what is going on. In particular we predict that as the temperature is lowered the crossover filling factor ν^* will be lowered and that the width of the peak region (in the filling factor) as well as the height of the the ZBC peak will increase. We also anticipate a region with the ZBC peak in spin conductance near $\nu \sim 2$ but not near $\nu \sim 1$. We find that there is more than one mechanism through which spin tunneling can happen, and depending on the channel, the spin tunneling may or may not be accompanied by charge tunneling.

Although in this paper we considered only the simplest possible case of a single tunneling center, it is interesting to investigate the effects of more than one impurity. While we have not investigated this problem extensively, it is clear that there should be interesting interference effects if there is more than one tunneling center. Indeed, some time ago Chamon and co-workers⁴⁴ proposed an experiment based on a two-tunneling-center device in the fractional quantum Hall regime as a way to measure the fractional statistics of Laughlin quasiparticles.

We finally note that there is a recent paper by Carpentier, Peca, and Balents⁴⁵ on a related problem. Carpentier and co-workers calculated the tunneling current between interacting Luttinger liquids constructed in a similar geometry as the geometry of the experiment by Kang and co-workers. They showed that electron fractionalization can be probed from multiple branch points of the current density. However, both the effect of charging (leaking) from (to) the bulk system and the absence of a chirality constraint make the system considered in the Ref. 45 quite different from the system considered in this paper in connection with the experiment by Kang and co-workers.

ACKNOWLEDGMENTS

We thank Professor W. Kang for several useful and stimulating discussions. This work was supported in part by the National Science Foundation through the Grant Nos. DMR98-17941 and DMR01-32990.

-
- ¹B. I. Halperin, Phys. Rev. B **25**, 2185 (1982).
²X. G. Wen, Phys. Rev. B **41**, 12 838 (1990).
³M. Stone, Phys. Rev. B **42**, 8399 (1990); Ann. Phys. (San Diego) **207**, 38 (1991).
⁴C. L. Kane and M. P. A. Fisher, Phys. Rev. B **46**, 15 233 (1992).
⁵C. L. Kane and M. P. A. Fisher Phys. Rev. Lett. **68**, 1220 (1992); **72**, 724 (1994).
⁶F. P. Milliken, C. P. Umbach, and R. A. Webb, Solid State Commun. **97**, 309 (1996).
⁷A. M. Chang, L. N. Pfeiffer, and K. W. West, Phys. Rev. Lett. **77**, 2538 (1996); M. Grayson, D. C. Tsui, L. N. Pfeiffer, K. W. West, and A. M. Chang, *ibid.* **80**, 1062 (1998); A. M. Chang, M. K. Wu, C. C. Chi, L. N. Pfeiffer, and K. W. West, *ibid.* **86**, 143 (2001).
⁸C. de C. Chamon and E. Fradkin, Phys. Rev. B **56**, 2012 (1997).
⁹A. V. Shytov, L. S. Levitov, and B. I. Halperin, Phys. Rev. Lett. **80**, 141 (1998).
¹⁰Ana López and Eduardo Fradkin, Phys. Rev. B **59**, 15 323 (1999).
¹¹J. Moore and X.-G. Wen, Phys. Rev. B **57**, 10 138 (1998).
¹²W. Kang, H. L. Stormer, L. N. Pfeiffer, K. M. Baldwin, and K. W. West, Nature (London) **403**, 59 (2000).
¹³T.-L. Ho, Phys. Rev. B **50**, 4524 (1994).
¹⁴A. Mitra and S. M. Girvin, Phys. Rev. B **64**, 041309 (2001).
¹⁵H. C. Lee and S. R. Eric Yang, Phys. Rev. B **63**, 193308 (2001).
¹⁶M. Kollar and S. Sachdev, Phys. Rev. B **65**, 121304(R) (2002).
¹⁷Y. Takagaki and K. H. Ploog, Phys. Rev. B **62**, 3766 (2000).
¹⁸K. Moon, H. Yi, C. L. Kane, S. M. Girvin, and M. P. A. Fisher, Phys. Rev. Lett. **71**, 4381 (1993).
¹⁹X. G. Wen, Phys. Rev. Lett. **64**, 2206 (1990); Phys. Rev. B **43**, 11 025 (1991); **44**, 5708 (1991).
²⁰W. Kang (private communication).
²¹See, for instance, by Michael Stone, *Bosonization* (World Scientific, Singapore, 1994), and references therein; V. J. Emery, in *Highly Conducting One-Dimensional Solids*, edited by J. T. Devreese *et al.* (Plenum Press, New York, 1979); A. O. Gogolin, A. A. Nersesyan, and A. M. Tsvelik, *Bosonization and Strongly Correlated Systems* (Cambridge University Press, Cambridge, England, 1998); David Sénéchal, cond-mat/9908262.
²²P. Fendley, A. W. W. Ludwig, and H. Saleur, Phys. Rev. B **52**, 8934 (1995); P. Fendley, A. W. W. Ludwig, and H. Saleur, Nucl. Phys. B **45**, 29 (1996).
²³H. Saleur, in *Topological Aspects of Low Dimensional Systems*, Proceedings of the 1998 Les Houches Summer School of Theoretical Physics, Haute Savoie, France, 1998, edited by A. Comet, T. Jolieur, S. Ouvry, and F. David (North-Holland, Amsterdam, 1998).
²⁴I. K. Affleck and A. W. W. Ludwig, Nucl. Phys. B **352**, 849 (1991).
²⁵J. Polchinski and L. Thorlacius, Phys. Rev. D **50**, 622 (1994).
²⁶N. Andrei, K. Furuya, and J. H. Lowenstein, Rev. Mod. Phys. **55**, 331 (1983), and references therein.
²⁷S. Goshal and A. Zamolodchikov, Int. J. Mod. Phys. B **9**, 3841 (1994).
²⁸A. W. W. Ludwig and I. K. Affleck, Phys. Rev. Lett. **67**, 3160 (1991); I. K. Affleck and A. W. W. Ludwig, *ibid.* **68**, 1046 (1992); Phys. Rev. B **48**, 7297 (1993).
²⁹Eduardo Fradkin, in *Quantum Physics at the Mesoscopic Scale*, Proceedings of the XXXIVth Rencontres de Moriond, Les Arcs, Haute Savoie, France, 1999, edited by C. Glattli, M. Sanquer, and J. Trânh Vân (EDP Sciences, Les Ulis, France, 2000); cond-mat/9905218.
³⁰U. Weiss, Solid State Commun. **100**, 281 (1996).
³¹M. P. A. Fisher and W. Zwerger, Phys. Rev. B **32**, 6190 (1985).
³²A. Koutouza, F. Siano, and H. Saleur, J. Phys. A **A34**, 5497 (2001).
³³See, for instance, Subir Sachdev, *Quantum Phase Transitions* (Cambridge University Press, Cambridge, England, 1998).
³⁴C. de C. Chamon, D. E. Freed, and X. G. Wen, Phys. Rev. B **51**, 2363 (1995); **53**, 4033 (1996).
³⁵See, for instance, Ana López and Eduardo Fradkin, Phys. Rev. B

- 63**, 085306 (2001), and references therein.
- ³⁶This decomposition has been used often in the literature. See, for instance, the reviews in I. K. Affleck, in *Fields, Strings and Critical Phenomena*, Les Houches Summer School on Theoretical Physics, (North-Holland, Amsterdam, 1990), Session XLIX.
- ³⁷G. Salis, D. D. Awschalom, Y. Ohno, and H. Ohno, Phys. Rev. B **64**, 195304 (2001).
- ³⁸See, for instance, P. Di Francesco, P. Mathieu, and D. Sénéchal, *Conformal Field Theory* (Springer-Verlag, New York, 1996); P. Ginsparg, in *Fields, Strings and Critical Phenomena*, Les Houches Summer School on Theoretical Physics, edited by E. Brézin and J. Zinn Justin (North-Holland, Amsterdam, 1990), Session XLIX.
- ³⁹D. J. Amit, Y. Y. Goldschmidt, and G. Grinstein, J. Phys. A **13**, 585 (1980).
- ⁴⁰This result is also well known from the g-ology literature. See, for instance, J. Sólyom, Adv. Phys. **28**, 201 (1979) and V. J. Emery's review cited in Ref. 21.
- ⁴¹A. Luther and V. J. Emery, Phys. Rev. Lett. **33**, 589 (1974).
- ⁴²F. D. M. Haldane, Phys. Lett. A **93**, 464 (1983); Phys. Rev. Lett. **50**, 1153 (1983); J. Appl. Phys. **57**, 3359 (1985).
- ⁴³This argument has been made by V. J. Emery, S. A. Kivelson, and O. Zachar, Phys. Rev. B **56**, 6120 (1997), in the context of the spin-gap proximity effect in striped superconductors.
- ⁴⁴C. de C. Chamon, D. E. Freed, S. A. Kivelson, S. L. Sondhi, and X. G. Wen, Phys. Rev. B **55**, 2331 (1997).
- ⁴⁵D. Carpentier, C. Peça, and L. Balents, Phys. Rev. B **66**, 153304 (2002).